7D.5 CONVECTION IN AN AFRICAN EASTERLY WAVE OVER WEST AFRICA AND THE EASTERN ATLANTIC: A MODEL CASE STUDY OF HURRICANE HELENE (2006)

Juliane Schwendike *

Karlsruher Institut für Technologie, Karlsruhe, Germany

1. INTRODUCTION

Mesoscale convective systems (MCSs), embedded in African easterly waves (AEWs) modulate the rainfall in West Africa and they are the seed disturbances for the development of tropical cyclones. There are still many unanswered questions concerning the interaction between AEWs and MCSs. It has been proposed that MCSs are important in the initiation of AEWs. However, the AEW troughs provide a favourable environment for the development of new MCSs. The manner in which the MCSs embedded in the AEW influence the AEW itself has been addressed only recently by very few studies.

In this study we contrast the different nature and evolution of MCSs over West Africa and the eastern Atlantic in one AEW to gain a better understanding of the interaction between the synoptic and the convective scale. Such differences have been investigated in previous studies. The novel aspect of our study is the direct comparison of convection over land and water within the same easterly wave and using the same model and diagnostic tools. We examine the net impact of convection on its environment as a first step towards examining the role of the convection in modifying the AEW. Over land, the convection takes the form of MCSs which move across West Africa. Over the ocean, the convection has the form of large convective bursts embedded in a cyclonic circulation that extends towards the surface. A number of MCSs may develop and decay within an AEW over the continent. Over the Atlantic, the organised convection within the AEW may develop into a tropical cyclone. By modelling the convection for one case we are able to compare and contrast the different properties. We analyse the relative vorticity budgets of the convective systems to address the question as to how the MCS modifies its environment.

2. MODEL

The **CO**nsortium for **S**mall scale **MO**delling (COSMO) non–hydrostatic limited–area numerical model[1] is used to simulate AEWs and embedded convective systems. The initial and boundary conditions for all runs are taken from 6–hourly European Centre for Medium Range Weather Forecasts (ECMWF) operational analyses. Three model runs are conducted for this study. The first is the COSMO run initiated on 9 September 2006 at 12 UTC with a horizontal resolution of 28 km that covers a domain from -60-20 °E and 0-45 °N. Two model runs with 2.8 km horizontal resolution were carried out such that the model region was centred around the MCS. Their model region comprise 19.5-1.025 °W 7.0-17.5 °N and 32.0-10.025 °W 5.0-16.975 °N, respectively. For the high–resolution model runs the parametrisation of convection is switched off. All the runs are 72–h in duration. This model setup includes 50 vertical levels. The top level in this study is at 20 hPa. The vertical resolution in the boundary layer is enhanced. The model source code was adapted to provide information for moisture, temperature and momentum budgets (Grams et al., 2010; Schwendike and Jones, 2010).

3. SYNOPTIC SITUATION AND COSMO SIMULATIONS

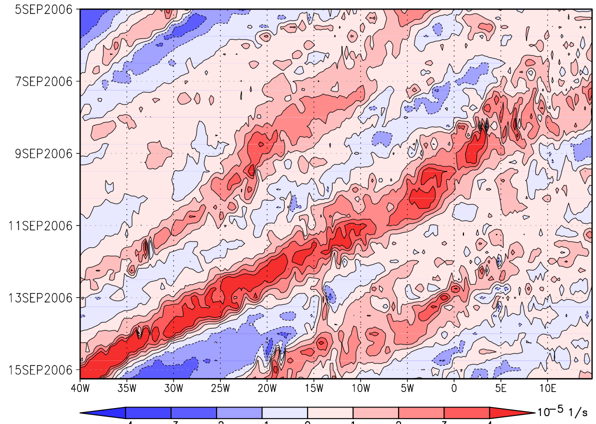

FIG. 1: The 700–hPa relative vorticity ($10^{-5}s^{-1}$) Hovmöller diagram from the ECMWF operational analysis between 5 September 2006, 00 UTC and 15 September 2006, 18 UTC. The relative vorticity is averaged between 6 °N and 16 °N. Taken from Schwendike and Jones (2010).

Our case study is the AEW out of which Hurricane Helene (2006) developed. It occurred in September 2006 during the special observation period of the African Monsoon Multidisciplinary Analyses (AMMA) project.

The AEW (Fig. 1) was generated in association with a large region of convection over the Highland of Ethiopia on 2 September 2006. The trough of the AEW is characterised by high relative vorticity. This AEW propagated westward across West Africa and reached 40 °W on 15 September 2006 at around midnight. Two additional AEWs with less intense vorticity maxima can be seen in Fig. 1 as well. The first one was initiated on 2

*Corresponding author address: Juliane Schwendike, Karlsruher Institut für Technologie, Kaiserstr. 12, 76131 Karlsruhe, Germany; e-mail: juliane.schwendike@kit.edu

[1]www.cosmo-model.org

September and reached 40 °W on 12 September, and the second wave was initiated on 6 September at about 38 °E and was located around 20 °W on 15 September. In the following we will focus on the AEW initiated on 2 September at around 33 °E, out of which Hurricane Helene developed.

At around 15 UTC on 9 September 2006, convection was initiated ahead of the trough of the AEW. The large–scale environment on that day was similar to that observed in Parker et al. (2005) except that the relatively moist monsoon flow had a very large westerly component and the African easterly jet (AEJ) had a very strong northeasterly component in the region where the convection occurred. The AEJ was located to the northwest of the convective system. The convective system grew rapidly into a mature MCS (Fig. 2a) which moved westwards across West Africa. As the convective system decayed a new convective burst occurred in the remains of the old system and a squall line formed at around 10 °W. The convection was enhanced as the system crossed the Guinea Highlands and it reached the West African coast line at around midnight on 10 September. Over the eastern Atlantic, this system decayed. On 11 September at around 00 UTC, a new convective system was triggered southeast of Dakar. It grew rapidly into a mature MCS over land and decayed as it crossed the West African coast. Afterwards, the convective activity was generally relatively low. A few hours later, several large convective bursts occurred (Fig. 2c) and by 12 UTC on 12 September the system was organised enough to be classified as a tropical depression. During this period the convection moved into the trough of the AEW and kept this position throughout the cyclogenesis. From this time on it is no longer the high positive relative vorticity of the AEW that can be seen in Fig. 1, but that of the strengthening Tropical Depression which moved westward within the trough of this AEW. On 13 September, convective banding began to increase in the northwestern part of the circulation. The convective system was upgraded to Tropical Storm Helene at 00 UTC on 14 September. Moving west–northwestward, Helene steadily intensified and became a hurricane at 12 UTC on 16 September. Helene continued to strengthen and became a category 3 storm on the Saffir–Simpson scale. Six hours later it reached its peak intensity with maximum sustained surface wind of about 54 m s^{-1}.

The Meteosat 8 infrared imagery and the model derived vertically integrated cloud ice, water vapour and humidity (henceforth, referred to as total water) are used to assess the ability of the high–resolution model runs to simulate the convective system. High values of total water, which indicate the convective updraught cores, are compared to the convective regions in the satellite images, highlighted by the orange–red colours. In general, the total water images indicate the convective updraught cores whereas the water vapour images illustrate the cirrus shield of the system (Fig. 2). However, we are still able to compare the size, the position and the shape of the convective systems.

A large MCS over Burkina Faso is evident in the COSMO run initialised at 9 September 2006 at 12 UTC. The leading edge of the convective system on 10 September 2006 at 04 UTC can be seen in Fig. 2b as a north south orientated band with an area of deep convection. The near–surface winds depict the mostly westerly monsoon flow. The regions with maximum total water content resemble the dark orange and black regions in the infrared images where a circularly shaped MCS is visible. The two regions of high total water in Fig. 2b are located in a similar position to the leading edge of the convective region in the infrared image (Fig. 2a). One hour later a third convective cell could be observed within the MCS.

Over the Atlantic the AEW moved over a large–scale southwest–northeast oriented monsoon trough with strong southwesterly flow to the southeast and subsequently a surge of northeasterly flow to the north (Fig. 2d). The character of the convective system changed. It was no longer one large MCS with either a circular or comma shape, but several large convective bursts occurred embedded in a mesoscale circulation. One example of these big convective bursts is shown in Fig. 2c, d. The model was able to capture these structure and intensity changes very well.

4. METHODOLOGY FOR BUDGET CALCULATION

The aim of this study is to investigate how the convective systems described above modify their environment and to relate these modifications to the structure of the convection itself. We assess the influence on the environment by calculating the vorticity budgets for regions encompassing the convective systems. These regions were determined according to the position and size of the system as follows. Firstly, a region of organised convection was identified using the vertically integrated specific humidity, cloud water and cloud ice. Budget calculations are carried out for boxes enclosing regions with values larger than 60 kg m^{-3}. If necessary, these boxes were enlarged so that they include also the regions with high vertical velocities ($|\omega| > 2$ Pa s^{-1}) related to the convective systems. The aim was to include the convective system during its lifecycle. Sensitivity experiments were carried out and it was found that the results of the budget calculation are not sensitive to the box size. The results changed by about 6% when the box size was increased by 50%. The profiles still had the same shape but were slightly smoothed.

The local change of the circulation C in the box is computed in pressure coordinates following Davis and Galarneau (2009):

$$\begin{aligned}\frac{\partial C}{\partial t} &= -A\overline{\eta}\widetilde{\delta} - \oint \eta'\vec{v}\cdot\vec{n}dl \\ &\quad + \oint \omega\left(\vec{k}\times\frac{\partial\vec{v}}{\partial p}\right)\cdot\vec{n}dl - \oint(\vec{k}\times\vec{F})\cdot\vec{n}dl,\end{aligned} \tag{1}$$

where η is the absolute vorticity, $\vec{v}$ is the horizontal wind speed, $\vec{n}$ is the unit vector normal to the boundary

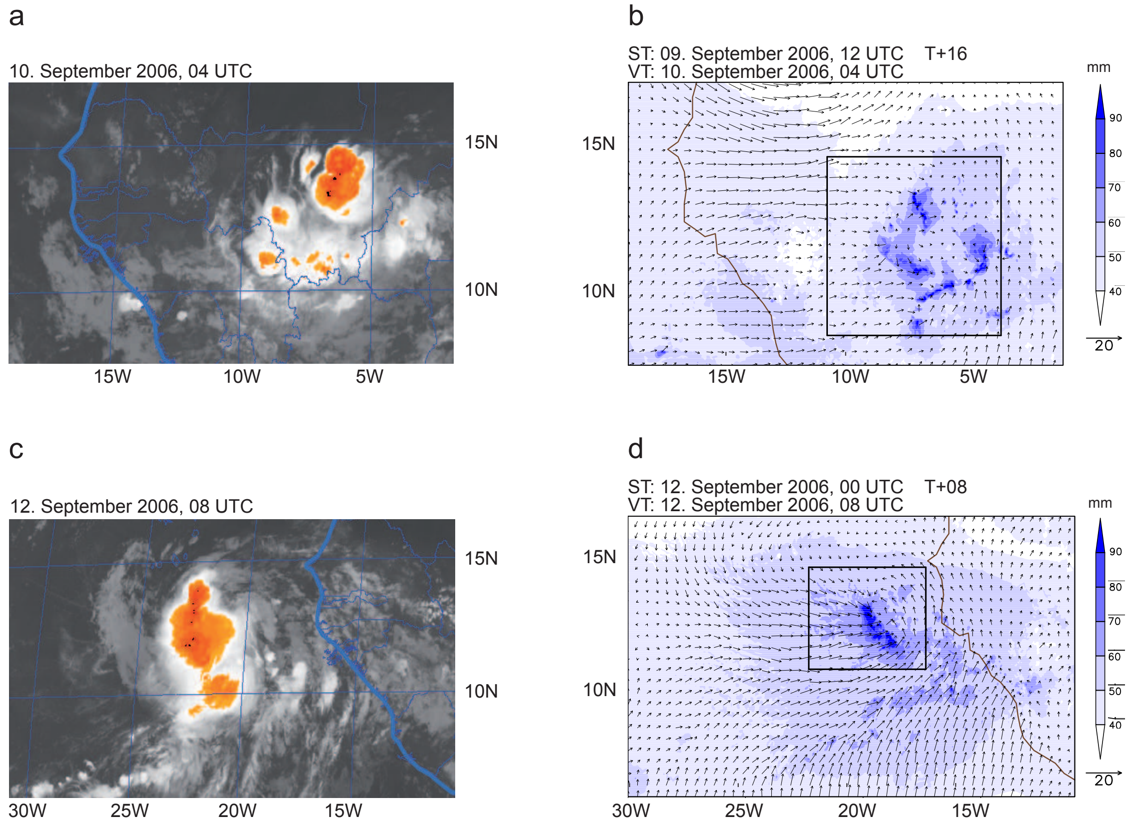

FIG. 2: Left column: Meteosat 8 infrared images (10.8 μm channel) where convective objects are superimposed using shadings of grey above -64 °C, orange–red colours between -64 ° and -82 °C, and black below -82 °C. Right column: The vertical integral of cloud water, cloud ice and humidity (kg m^{-2}) as well as the horizontal wind (m s^{-1}) at 975 hPa based on the 2.8–km COSMO runs are shown at selected stages of the life cycle of the convective systems at the date and time given above the image. ST denotes the starting time of the simulation, and VT denotes the verification time. The subplots a, b correspond to model run 2, c and d is a section of model run 4. Taken from Schwendike and Jones (2010).

of the closed region, ω is the vertical velocity in pressure coordinates (x, y, p), $\vec{k}$ is the unit vector in the vertical, and $\vec{F}$ is the frictional force. The overbars define the average value around the perimeter of the box, the primes denote the deviation from this value, and the tildes indicate the average over the area of the box. The first term on the right hand side (henceforth rhs) is the mean stretching term consisting of the product of the average values of vorticity $\overline{\eta}$ and divergence $\tilde{\delta}$ over the area A. The second term on the rhs is the eddy flux term which can increase the circulation within the box if inward flow is correlated with positive vorticity perturbations and outward flow with negative vorticity perturbations. This term is identified with the horizontal vorticity advection. The third term on the rhs describes vortex tilting and the fourth term friction. Friction was neglected in the relative vorticity budget. Even without it the budgets are nearly balanced. The budgets were not calculated below 950 hPa because in some regions in the domain the levels below 950 hPa are below ground level. Additionally, the neglect of friction is unjustifiable so close to the surface.

5. CONVECTIVE SYSTEMS OVER WEST AFRICA AND THE ATLANTIC

We focus on two convective systems embedded in the same AEW: one over the West African continent and the other over the eastern Atlantic. Three different stages of the life cycle of the MCS over West Africa are identified: the growing phase, the mature stage and the dissipating stage. The evolution of the convective burst over the Atlantic was divided into the growing and the decaying phase. During the mature stage of the MCS over land and during the growing stage of the convective system over the ocean, East–West cross sections where taken through the systems (Fig. 3) to illustrate their similarities and differences.

During the mature phase of the convective system over the land (Fig. 3a) low–level convergence occurs between a strong westerly inflow and an easterly flow from behind the system. The westerly inflow reaches deep into the system up to 550 hPa. The region of strong divergence occurs at the leading edge of the convective system between about 800 and 400 hPa and is tilted with height. Divergence associated with the upper–level out-

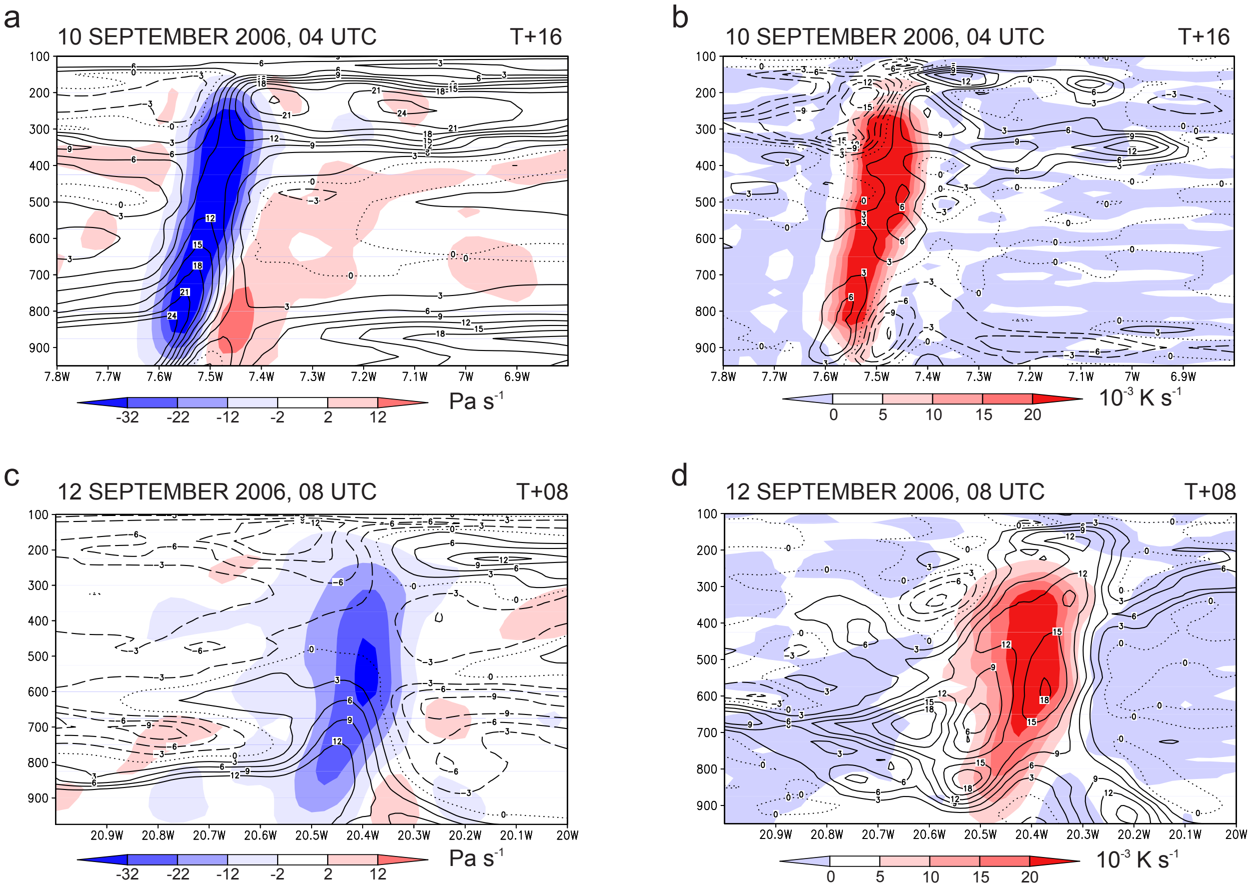

FIG. 3: Cross sections through the convective system over West Africa of (a, c) vertical velocity (shaded) and system–relative zonal wind (contour interval is $3\,\mathrm{m\,s^{-1}}$) and (b, d) total diabatic heating rate (shaded) and the vertical component of the relative vorticity (contour interval $3\times10^{-4}\,\mathrm{s^{-1}}$) based on the COSMO run initiated at 12 UTC on 9 September 2006. The convective system moved westwards with a translation speed of about $12.2\,\mathrm{m\,s^{-1}}$ during the developing stage (a,b), $15.3\,\mathrm{m\,s^{-1}}$ during the mature stage (c,d) and $10.7\,\mathrm{m\,s^{-1}}$ during the decaying stage (e,f). The cross sections (a,b) are along 13.5 °N at T+13 in box A, (c,d) along 13.1 °N at T+16 in box B, and (e,f) along 12.3 °N at T+22 in box C. Pressure (hPa) is used as the vertical coordinate. Taken from Schwendike and Jones (2010).

flow can be seen at around 250 hPa with stronger westerly winds to the rear and weaker easterly winds ahead of the system. Thus there is strong mid–level convergence east of the tilted updraught. The region of maximum heating (Fig. 3b) is collocated with the region of the strongest ascent. The low–level convergence is intensified due to the descending air from the rear of the system. At this stage strong downdraughts have developed around 7.5 °W behind the tilted updraught where a zonal system–relative wind minimum is located just behind the the low–level convergence zone characterised by a wind maximum at around 7.7 °W. The downdraught region is characterised also by a very weak cooling. Between 200 and 300 hPa, the strongest outflow from the system is to the east and weaker outflow to the west (Fig. 3a) giving a region of strong outflow that extends about 100 km. An elongated horizontal band with negative relative vorticity develops through vortex compression in the region of strong divergence and is then advected to the west. This negative vorticity anomaly is seen along the upper–level region of strong outflow in each system. Positive relative vorticity that develops through vortex stretching in the vortex core is advected upwards and towards the east in the tilted updraught, leading to an upper-level vorticity dipole (Fig. 3b). A dipole of opposite sign occurs at low–levels but this appears to develop due to vortex stretching in the updraught region and vortex compression in the region of the strong downdraughts. Below 400 hPa weaker descent occurs. The easterly system–relative wind speed maximum at around 450 hPa ahead of the convective system can be related to air that came from the inflow region, was lifted upwards and then exited the convective region at about 450 hPa or slightly lower. The weakly subsiding air leads to an enhancement of the AEJ. This was evident from trajectory calculations.

The convective system over the ocean at a time close to its peak intensity is shown in Fig. 3c,d. The northern convective burst at the beginning of the period shown still displays some MCS–like character, as it has a bow–like form, moves toward the west and develops weak downdraughts. It occurs in a region that is close to the AEJ, which is located to the northwest. Thus the shear profile is similar to that of the MCS over West Africa. However, the region of maximum heating and ascent is only tilted below 700 hPa (Fig. 3a,b) rather than through its entire depth, as in the convective system over land and is collocated with a deep tower of positive vertical vorticity, so that this convective system could be described as a vortical hot tower. It is evident that the upper level outflow is much weaker and covers a smaller region than over land. Additionally, the downdraughts are weaker and smaller–scale than for the system over land.

The convection embedded in the AEW over land and over the ocean exhibits rather different structural characteristics. Differences occur also in the environment of both convective systems. The mean relative humidity was calculated for a region encompassing all the convective systems described above over land and for a region around the convective system over the ocean (Fig. 4). The atmosphere is markedly dryer over land than over water. In particular, the mid–level relative humidity (700-500 hPa) is noticeably lower over land. The MCS over land redistributes the moist air from lower levels to mid–levels. Inspection of the evolution of the moisture profiles over land (not shown) indicates that the moistening of the mid troposphere is particularly marked during the period illustrated in Fig. 2a,b as the MCS develops to its mature phase. Over the ocean the redistribution of moisture continues during the frequent sequence of convective bursts over the Atlantic. The evolution of the moisture profiles is consistent with the drier air at mid–levels leading to stronger downdraughts over land.

Over land, the maximum mean zonal wind with values of about -15 $\mathrm{m\,s^{-1}}$ (Fig. 4b) occurs at around 600 hPa, which is due to the AEJ. As the convective systems grow, the magnitude of the mid–level mean zonal wind maximum decreases whereas the magnitude of the low–level mean zonal wind maximum at around 900 hPa increases, as the low–level inflow into the convective system strengthens. After 25 hours into the simulation the wind speed below 800 hPa is lower than after 7 hours. The height of the mid–level wind maximum is reduced with time but the influence of the AEJ is still apparent. However, the shear is reduced between 800 and 600 hPa but increased below this layer. The profile of the mean zonal wind is similar over land and over the ocean, although the wind speed maximum at low–levels over the ocean does not change with time and the zonal wind maximum at around 600 hPa reached values if about 12 $\mathrm{m\,s^{-1}}$ (Fig. 4c). The mid–level wind speed decreased with time in such a way that only very weak vertical shear occurs above 800 hPa ofter 13 forecast hours, in contrast to the land case.

The stronger influence of the AEJ on the system over land than on the system over the ocean might be due to the fact that the MCS over West Africa was initiated ahead of the AEW trough, where it remained throughout its lifetime. As the convective systems moved over the Atlantic they also moved into the AEW trough. The low–level flow is similar in strength over land and ocean, but the AEJ is stronger over land leading to a stronger vertical shear in the early stage of convection over land than over the ocean. Additionally, the shear is much weaker toward the end of the life–cycle of the convective system over the ocean than to the beginning. In contrast, the shear over land did not change as much.

The convective available potential energy (CAPE) is spatially variable over land and over water. Both systems formed in an area with high values of CAPE, of around 1500-2000 $\mathrm{J\,kg^{-1}}$. High values of CAPE were always present ahead of the systems.

A distinct cold pool developed during the life cycle of the MCS over land (Fig. 5) as a result of the storm's downdraught. The cold pool spreads out as a density current with a leading edge that can be seen in the strong potential temperature gradient in Fig. 5. Over water no cold pool was observed. The downdraughts of the convective system over the ocean (not shown) appear to be not as strong as in the MCS over land (Fig. 3a) and there is no distinct cold pool over the eastern Atlantic. Thus there is no mechanism for the convective systems to propagate. The vertical shear over the ocean is about 75% of that over land at the beginning of the period we discuss and decreases substantially over the 8 hour period shown (Fig. 4). Initially, the convective updraught over the ocean is tilted at low levels (Fig. 3c,d) but becomes more upright with time as the vertical shear decreases. Both the lack of cold pools and the decrease in shear with time make it more difficult for the convection to be long–lived resulting in a shorter life time. The environment, however, is favourable for new convection. Thus, over the Atlantic there are more convective systems with a moderate intensity rather than a large long–lived mesoscale convective system.

6. VORTICITY BUDGET

In order to assess how the structural differences described previously impact the dynamics of the systems, we contrast the evolution of the relative vorticity for the convective systems over land and over water embedded in the same AEW. The relative vorticity budget for convection over land and over water was computed based on hourly model output. The overall balance of the relative vorticity budget is good (not shown). Some discrepancies occur near the surface and at around 800 hPa over land. Note that rhs is the sum of all terms except friction in equation 1, which gives the tendency of the circulation averaged around a box.

The low–level vorticity is much higher over the ocean than over land (Fig. 6a, b) due to a low–level vorticity anomaly that moved into the box region (not shown). This vorticity anomaly is in fact a secondary heat low that moved over the Atlantic. On 9 September 2006 at 12 UTC a westward extension of the Saharan heat low core occurred. It moved over West Africa along about 18 $^\circ$N. A shallow circulation confined to the 1000–800 hPa layer became cut off from the main Saharan heat low and is re-

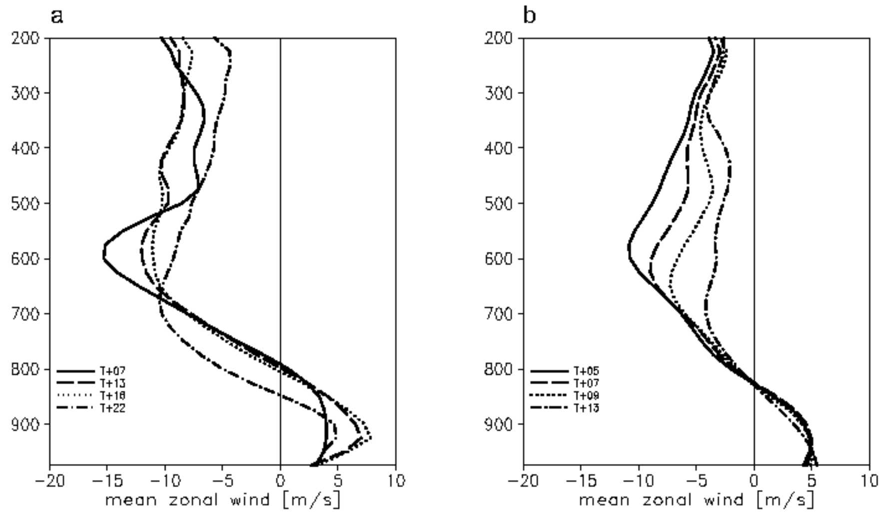

FIG. 4: (a) Solid line: Mean relative humidity of the convective system over land averaged over 8.5-14.5 °N, 11.0-5.4 °W from 9 h to 24 h forecast time, based on the COSMO run initialised on 9 September 2006, 12 UTC. Dashed line: Mean relative humidity for the convective system over the eastern Atlantic averaged over 10.5-14.0 °N, 22.5-17.5 °W, from 7 h to 15 h forecast time, based on the COSMO run initialised on 12 September 2006, 00 UTC. (b) Mean zonal wind for the convective system over West Africa averaged over 8.5-14.5 °N, 11.0-5.4 °W based on the COSMO run initialised at 12 UTC on 9 September 2006, are displayed for selected times. (c) Mean zonal wind for the convective system over the eastern Atlantic averaged over 11.0-13.8 °N, 21.2-18.0 °W, for different times. Pressure (hPa) is used as the vertical coordinate. Taken from Schwendike and Jones (2010).

ferred to as a secondary heat low. Further inspection of the model wind, temperature and humidity fields confirm the heat–low character of this circulation. The low level temperature maximum was collocated with the maximum of positive relative vorticity. The flow above the secondary heat low was predominantly easterly, associated with the AEJ. The enhanced vorticity in the AEW trough was located further inland. The secondary heat low crossed the West African coastline in the evening hours of 11 September. The secondary heat low moved southwestwards over the ocean and retained warmer temperatures compared to its environment. On 12 September at 00 UTC it started to move into the box over the ocean. Thus the initial enhanced low–level vorticity over the ocean occurred due to both the secondary heat low and the monsoon circulation. At this time the convective activity over the Atlantic was very low. At 600 hPa, the AEW moved into the box from the east. Six hours later the low–level and the mid–level vorticity maxima began to overlap each other. This is the time when convection is initiated over the Atlantic and the tropical depression starts to develop.

Different processes attain importance during the life cycle of the MCS over West Africa and the convective system over the eastern Atlantic. The hourly rate of change of the average relative vorticity over land (Fig. 6a) peaks after 18 hours just below 700 hPa and below 800 hPa. Above 400 hPa the relative vorticity decreases. The MCS over land consisted of 3 prominent convective systems with different stages of maturity. At the beginning of the period considered the three systems developed very quickly. During these two hours a positive relative vorticity tendency occurs below 700 hPa due to stretching and a weakly negative tendency occurs above. As the MCS grows, the vertical vorticity tendency due to stretching increases in magnitude (Fig. 6c) and the depth of the layer with vortex stretching increases with time. By the end of the period shown vortex stretching extends up to 600 hPa and has the strongest impact on the net relative vorticity change below 700 hPa. The convective system developed a distinct divergent outflow. Thus, there is vortex compression above 600 hPa. The strongest effect of tilting is mainly restricted to the levels between 800 and 900 hPa. During the system's life cycle the height of the maximum negative tendency due to tilting decreases. Tilting has only a small contribution at mid–levels. Above 600 hPa, the tendency due to tilting is only slightly positive. A large impact at mid–levels results from the eddy flux. As we will see later this presents a striking difference to the relative vorticity budget over the ocean.

The eddy flux or horizontal advection of relative vorticity is largest at the height of the AEJ and positive between 450 and 750 hPa (Fig. 6b), especially during the first 3 hours and then again after a forecast time of 17 hours. The relative vorticity tendency due to the eddy flux is negative below about 850 hPa (Fig. 6b). This negative tendency becomes stronger with time. Thus the main contribution to the increase in average vorticity is the eddy flux term. For the area over which the budget was calculated the main contribution to the eddy flux appears to be from anomalously positive vorticity being advected inwards at the northeast corner of the box. Three main features influence the eddy flux for the convective

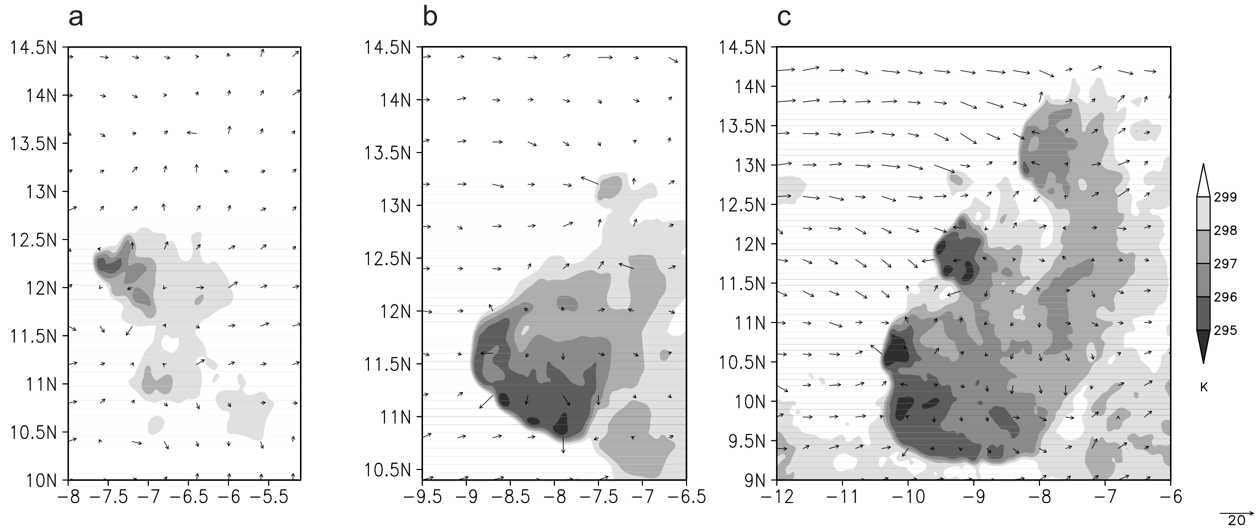

FIG. 5: Potential temperature (K) and the horizontal wind ($m\,s^{-1}$) at 975 hPa for (a) T+13, box B (b, T+16) and box C (c, T+22) based on the COSMO run initialised on 9 September 2006, 12 UTC. Taken from Schwendike and Jones (2010).

system over West Africa: the AEJ / AEW, the secondary heat low northwest of the box and the system itself.

The situation over the ocean is rather different (Fig. 6e-h). The relative vorticity tendency is strongly positive between the forecast hours 5 and 8 and the height of the maximum relative vorticity tendency decreases significantly (Fig. 6e). Between 600 and 450 hPa the relative vorticity tendency is negative, becomes stronger with time and moves downward. The decreasing height of the maximum relative vorticity tendency is due to the decrease in height and intensity of the tendency due to eddy flux. Over water, the AEW at 600 hPa moves through the box for which the relative vorticity budget was calculated. The evolution of the eddy flux over water (Fig. 6f) appears to be dominated by two factors. The first one is the advection of positive absolute vorticity anomalies at the eastern boundary into the box and the advection of negative perturbation absolute vorticity out of the box at the western side. This is responsible for the initial strongly positive tendency. The second factor is an area of positive absolute perturbation vorticity in the southern portion of the box (not shown). Depending on the flow pattern at the southern boundary this anomaly is at times advected into the box and at other times out of the box. At the southern side of the box, between 550 and 300 hPa, positive absolute vorticity is advected into the box as the results of the outflow of convective systems south of the box analysed here. Due to the related vorticity anomalies the eddy flux results in a positive relative vorticity tendency between 600 and 800 hPa during 8 hours into the simulation and a negative tendency during the next 4 hours (Fig. 6f).

As the system grows, the low–level convergence becomes much stronger and reaches its peak intensity during the system's growing and early maturing phase (T+6 to T+10). This results in a strong positive relative vorticity tendency below 700 hPa. The divergence aloft accounts for the negative relative vorticity tendency. At around 12 hours into the simulation, a positive relative vorticity tendency can be observed between 300 and 400 hPa and around 500 hPa, which can be attributed to convergence in the region where stratiform clouds occur. The downdraught at midlevels and the stratiform region above give the mid–level vortex compression and upper level stretching. The tilting term plays a minor role in the relative vorticity budget. The effect of tilting is weakly positive, in contrast to the system over land, and is found at lower levels when small convective cells occur at the boundary of the box. The vorticity budget over the ocean illustrates nicely how the tropical cyclogenesis occurs as the AEW moves into the box (Fig. 6f) and the subsequent convective events in an environment with preexisting cyclonic vorticity enhance the low–level vorticity (Fig. 6g). A distinguishing feature of this case is the role of both the heat low and the monsoon flow in creating the low–level cyclonic environment.

7. SUMMARY

We contrasted a convective system over West Africa and one over the eastern Atlantic, both embedded in the AEW out of which Hurricane Helene developed. Over land the MCS had a lifetime of several days, whereas over the ocean intense convective bursts occurred. The largest and long lived convective burst in this intensification period was analysed here and compared to the MCS over land.

The main difference between both convective systems is that the one over land is tilted, and the one over the ocean is upright above 700 hPa. For both systems the region with the strongest updraughts is collocated with the region of maximum diabatic heating. The downdraughts led to the development of cold pools over land. The CAPE in the environment of both convective systems

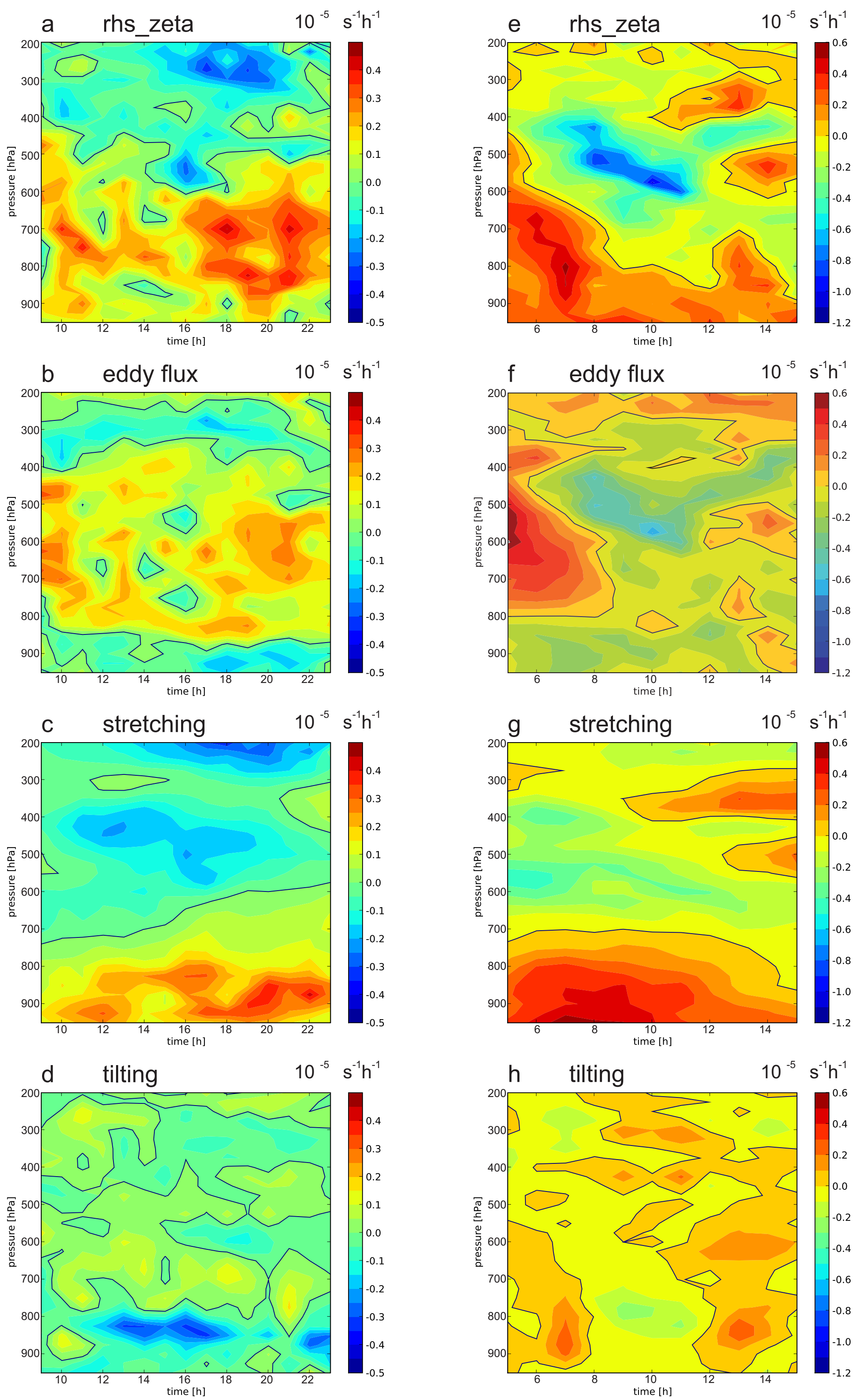

FIG. 6: (a)-(d): Time–pressure series of hourly changes in box–averaged vorticity representing (a) total relative vorticity tendency (neglecting friction), (b) eddy flux, (c) stretching, and (d) tilting for the MCS over West Africa. The box (11.0 to 4.0 °W, 8.5 to 14.5 °N) encompasses the convective system throughout the whole time. The forecast hours are shown here based on the model run that was initiated on 9 September 2006, 12 UTC. (e)-(h): As in (a)-(d), but averaged over 23.0-17.5 °W and 10.5-14.5 °N for the convective burst over the Atlantic. This model run was initiated on 12 September 2006, 00 UTC. Note, the colour scale is different over land and water. The black contour denotes the zero–line. Taken from Schwendike and Jones (2010).

is similar. The shear between 600 and 800 hPa over land is significantly larger than over the ocean. There is hardly any shear at mid–levels over the ocean and the influence of the AEJ is reduced but still apparent over land. Drier air at mid–levels over land leads to stronger downdraughts and to strong cold pools which propagate and thus help the convection to grow into a mature MCS. Over the ocean, the mid–level air is moister, weaker downdraughts occur and no cold pool develops. Without a cold pool there is no mechanism for the convective system to propagate and thus the oceanic convective systems remain smaller. Due to the smaller shear especially towards the end of the analysed period the convection is harder to sustain and the lifetime is shorter. The environment, however, is favourable for new convection to form. This leads to the succession of smaller convective systems instead of a single, large MCS over land.

Over land, the relative vorticity increased from about 900 to 500 hPa and decreased above 400 hPa. Over the ocean, the relative vorticity between 600 and 400 hPa is relatively high at the beginning of the observation period and increased up to a forecast time of 9 h. During the following hours the vorticity increased only slightly but the height at which the maximum occurred was lowered significantly. The main reason for the total relative vorticity changes is the tendency due to stretching over the ocean and the eddy flux over West Africa where it led to an increase in vorticity at mid-levels. The tendency due to stretching leads to a negative relative vorticity tendency above 600 hPa over land and over the ocean. It had a positive contribution at low-levels as well as between 300 and 500 hPa towards the end of the analysed period of the convective system over the ocean. The second important component in the relative vorticity budget is the eddy flux. It has a positive tendency at the beginning and towards the end of the observation period for the system over land. Over the ocean it had its strongest effect at the very beginning of the life cycle of the convective system. Its effect decreased as the system reached maturity but positive tendencies occur at midlevels towards the end. The tilting term lead to a mostly negative tendency in the lower troposphere, but provided the smallest contribution to the relative vorticity budget as also shown by other studies. Over the ocean, the increase in relative vorticity and hence potential vorticity was lowered markedly and much stronger than for the system over land. This process plays an important role in the cyclogenesis of Hurricane Helene. During the period analysed over the ocean the convective system was classified a tropical depression.

ACKNOWLEDGEMENT

Based on a French initiative, AMMA was built by an international scientific group and was funded by a large number of agencies, especially from France, UK, US and Africa. It has been the beneficiary of a major financial contribution from the European Community's Sixth Framework Research Programme. Detailed information on scientific coordination and funding is available on the AMMA International web site http://www.amma-international.org. Radiosoundings from the stations Bamako and Dakar were made available due to the efforts of Jean-Blaise Ngamini and his team at ASECNA.

We are grateful to Leonhard Gantner for assisting with COSMO and to Christian Grams for providing code for the potential temperature budget. We are obliged to Leonhard Scheck for his technical and general support. We would like to thank Andreas Schmidt for creating the Meteosat images. This work benefited from discussions with Chris Davis, Patrick Harr, Jean-Philippe Lafore, David Nolan, Frank Roux and Uli Blahak.

REFERENCES

Davis, C. A. and T. J. Galarneau, 2009: The vertical structure of mesoscale convective vortices. *J. Atmos. Sci.*, **66**, 686–704.

Grams, C. M., S. C. Jones, J. Marsham, D. J. Parker, J. M. Haywood, and V. Heuveline, 2010: The Atlantic inflow to the Saharan heat low: observations and modelling. *Q. J. R. Meteorol. Soc.*, **136(s1)**, 125–140.

Parker, D. J., C. D. Thorncroft, R. Burton, and A. Diongue-Niang, 2005: Analysis of the African easterly jet using aircraft observations from the JET2000 experiment. *Q. J. R. Meteorol. Soc.*, **131**, 1461–1482.

Schwendike, J. and S. C. Jones, 2010: Convection in an African Easterly Wave over West Africa an the eastern Atlantic: a model case study of Helene (2006). *Q. J. R. Meteorol. Soc.*, **136(s1)**, 364–396.